JOTCSA, Volume 3, issue 2, (2016), pp. 183-206. **Research article**

Journal homepage: http://dergipark.ulakbim.gov.tr/jotcsa

e-ISSN: 2149-0120

Structural Characterization and Gas Permeation Properties of Polyetherimide (PEI)/Zeolitic imidazolate (ZIF-11) Mixed Matrix Membranes

Mehtap ŞAFAK BOROĞLU[1]*

[1]Department of Chemical Engineering, Faculty of Engineering, Istanbul University, Istanbul, Turkey.

Abstract: In this study, the preparation of polyetherimide (PEI-Ultem1000)/ZIF-11 mixed matrix membranes was studied in various ZIF-11 particle loadings (0, 10, 15, 20, and 30 wt.%). The newly synthesized ZIF-11 submicron particles with an average particle size of ~280 nm were integrated in PEI membranes as novel mixed matrix membranes (MMMs). The effect of ZIF-11 loading was scrutinized for H_2, CO_2, and CH_4 gas separation performances at 35 °C and 4 bar. The incorporation of ZIF-11 submicron particles improved the gas permeation properties of the MMMs with an increase in ZIF-11 loading. As the ZIF-11 loading increased up to 20 wt.%, the permeability of H_2 and CO_2 increased to four times higher than that of the pure polymer. Moderate increase of CH_4 permeability was also recorded. At higher loadings above 20 wt.%, the permeability decreased for all gases and the CO_2/CH_4, and H_2/CH_4 selectivities increased consistent with the ZIF-11 loading.

Keywords: Metal organic frameworks, zeolite imidazolate frameworks, polyetherimide, gas separation.

Submitted: May 28, 2016. **Revised:** June 24, 2016. **Accepted:** June 28, 2016.

Cite this: ŞAFAK BOROĞLU M. STRUCTURAL CHARACTERIZATION AND GAS PERMEATION PROPERTIES OF POLYETHERIMIDE (PEI)/ZEOLITIC IMIDAZOLATE (ZIF-11) MIXED MATRIX MEMBRANES. Journal of the Turkish Chemical Society, Section A: Chemistry. 2016;3(2):183–206.

DOI: 10.18596/jotcsa.62047.

Correspondence to: Mehtap ŞAFAK BOROĞLU, e-mail: mehtap@istanbul.edu.tr.

INTRODUCTION

The gas separation by membranes is an active and rapidly growing research area. In membrane-based gas separation processes, components are separated from their mixtures by differential permeation through membranes. Some technologies (*e.g.* distillation and absorption processes) prescribe a phase change in the mixture. The change of this phase adds a significant energetic disadvantage. On the other hand, gas separation by the membrane does not necessitate a phase change (1). The gas separation membrane market has grown significantly and continued progression is expected to escalate in the coming years as technology improves and applications are multiplied (2). Membrane technology for gas separation has been carried out in a variety of applications, such as, oxygen, nitrogen enrichment, hydrogen recovery, and natural gas dehydration (3). However, the development of polymeric membrane separation technology has been necessitated by a so-called performance upper bound in the trade-off curve between the gas permeability and selectivity (4). Permeability and selectivity trade-off for gas pairs were well illustrated in the so-called Robeson Plots (5). There is tremendous research effort to surpass Robeson trade-off limit curve by adding creative additives into appropriate polymeric material (6). Addition of synthetic nanoparticles compatible with polymers, known as mixed matrix membranes (MMMs), was the one of the approaches to advance membrane separation processes (7,8). MMMs combine the potential advantages of both inorganic particles and organic polymer membranes, such as, superior permeability and selectivity of the inorganic particles with good processability and mechanical properties of the polymer membranes (9). MMMs which were prepared from different inorganic and organic materials produced superior separation performance due to the incorporation of synthetic molecular sieves and Metal Organic Frameworks (MOFs) are a relatively new class of microporous materials, and consist of transition metals and transition metal oxides connected by organic linkages to create one-, two- and three-dimensional microporous structures (10). The recent development in the synthesis of MOFs led to the promising applications as drug delivery carriers, storage media, adsorbents for separations, and catalysts (11–13). They have large surface area, affinity towards certain gases and controlled porosity (14). The main advantage of MOFs over well-known nanoporous materials was the ability to arrange their chemical and physical properties during synthesis process by changing the combination of metals and organic linkers (15). Zeolitic imidazolate frameworks (ZIFs) have received world-wide attention to enhance MMMs' compatibility and permeability (16). Several ZIFs have been synthesized in the literature and considered as potential candidates for gas separations due to the diversity in their pore sizes, higher thermal and chemical stability compared to zeolites and other MOFs (17). Yaghi and co-workers have developed various zeolitic topologies, such as rhombic dodecahedron (RHO) and sodalite (SOD) topologies (18). Particularly, several ZIFs have been successfully prepared to be incorporated into mixed matrix membranes. ZIF-8 type metal organic framework was the most widely used one and reported due to the enhanced membrane performances (19). Selfert and co-workers showed that ZIF-11 has exceptional thermal and chemical properties and ZIF-11 has bigger H2 adsorption energies than that on ZIF-8 (20). Keskin *et al.* reported that ZIF-11 was settled above the upper bound because of higher CO_2 selectivity (>100) and permeability (104−105 Barrer). Molecular simulation results showed that this high CO_2 selectivity resulted from the large differences in diffusion rates of CO_2 and CH_4 gases in the ZIFs' pores (17).

ZIF-11 has been obtained through solvothermal synthesis by using diethylformamide (DEF) as solvent (21). RHO type zeolite structure ZIF-11 has larger cavities of 14.6 Å connected with the pore apertures of 3.0 Å. These preferable properties make it suitable for H_2 separation (Figure 1) (22). Difficulties in removing DEF from the pores of ZIF-11, Wang *et al.* studied a new synthetic method at room temperature by using methanol as solvent and toluene as the structure template (23).

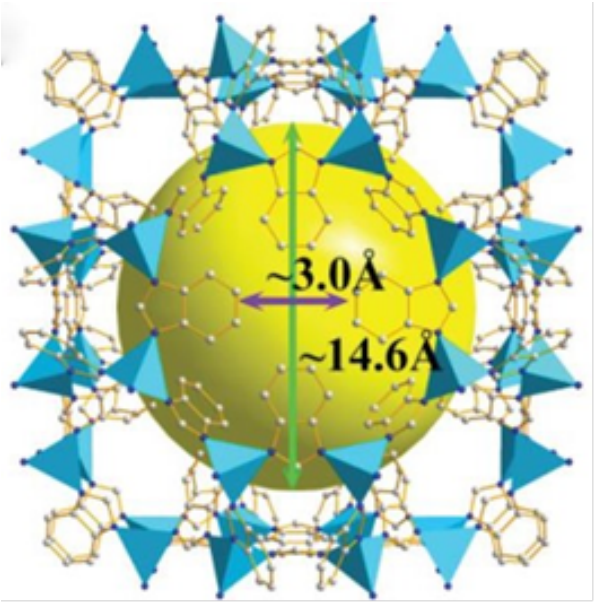

Figure 1. Crystalline structure of ZIF 11 (RHO) particle (23).

Commercial polyetherimide (PEI-Ultem1000) has several important advantages as an organic membrane material. As one of them, PEI has high diffusivity selectivity provided by their rigid backbones and fused ring structures. These properties render them attractive in polymeric membrane developed for gas separations. PEI's glass transition temperature was 216 °C and high T_g temperature allowed the usage of higher pressures and temperatures in applications without plastic deformation. The studies on gas permeation of the PEI dense films revealed that PEI exhibited high selectivity for many important gas pairs especially He and H_2 separation from other gases (24).

In this work, ZIF-11 particles were synthesized and used as filler, and PEI (Ultem 1000) as the continuous phase were utilized to prepare MOF-based mixed matrix membranes for CO_2/CH_4, H_2/CH_4, H_2/CO_2 separation. The separation performance of these MMMS as a function of ZIF-11 loading in the PEI matrix was systematically investigated. The thermal, morphological, and gas separation properties of the synthesized membranes have been investigated using XRD, FTIR, SEM, TGA, DSC, and single gas permeation setup.

MATERIALS AND METHODS

Materials

Polyetherimide (Ultem® 1000) was purchased from Sigma Aldrich, Germany. Typical chemical structure of PEI and some properties were shown in Figure 2 and Table 1. Zinc acetate dihydrate ($C_4H_6O_4Zn.2H_2O$, ≥98%, Sigma-Aldrich, USA) was used as a source of zinc. Benzimidazole ($C_7H_6N_2$, BIm, > 98%, Sigma-Aldrich, Germany) was the primary ligand used. Ammonium hydroxide (NH_3, min. 25% aqueous solution) was purchased from Lachema, Czech Republic and all chemicals were used without further purification. N-Methyl-2-pyrrolidone (NMP, >99.5%), methanol (for analysis) and toluene (>99.9%) were purchased from Merck. Single gases used in the permeation experiments were carbon dioxide (CO_2), methane (CH_4) and hydrogen (H_2) of gas chromatographic grades (purities >99.8 %) from Linde Gas Company (Linde Gaz, Turkey). The properties of gases are given in Table 2.

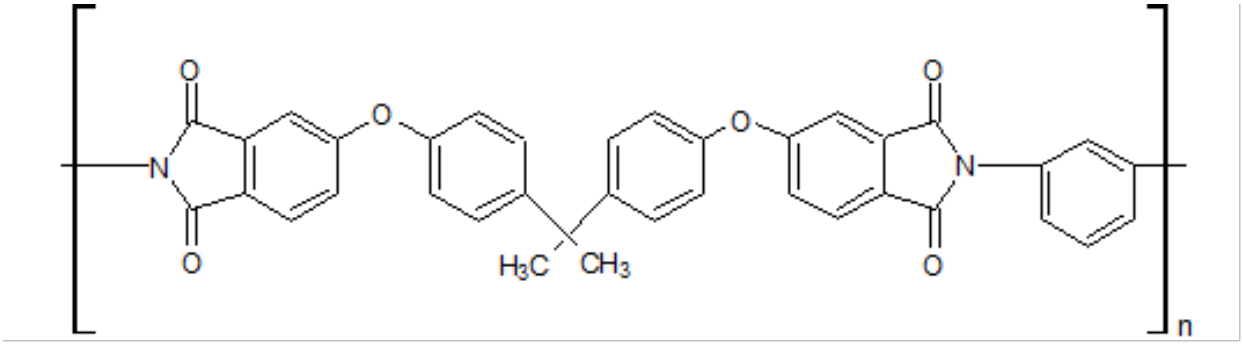

Figure 2. The chemical structure of PEI (Ultem 1000).

Table 1. Physical properties of unmodified PEI (Ultem 1000).

Properties	Symbol	Value
Molecular weight (kg/kmol)	M_w	55,000
Glass Transition Temperature (°C)	T_g	216
Density (kg/m^3)	d	1270
Melting Point (°C)	T_m	219

Table 2. Properties of H_2, CH_4 and CO_2.

Gases	Critical temperature (K)	Critical Volume (cm^3/mol)	Kinetic diameters (nm)
H_2	33.20	64.9	0.289
CH_4	190.6	98.6	0.380
CO_2	304.2	91.9	0.330

EXPERIMENTAL PROCEDURE

Preparation of ZIF-11 particles

The recipe for the synthesis of ZIF-11 powder was a modified version of the method developed by the Wang and Yaghi group (23,25). In the synthesis of ZIF-11 submicron particles, 4.8 g of BIm (4 mmol) was dissolved in 16.61 g of methanol, followed by the addition of 20.88 g of toluene (226.6 mmol). 0.14 g of NH_3 (aq) (4.014 mmol) was added into the solution at room temperature. 4.4 g of zinc acetate dihydrate (20 mmol) was added and stirred for 2 h at room temperature to complete the crystallization step. The final solution had a Zn: BIm : NH_3 : C_2H_5OH : toluene molar composition of 1 : 2 : 2 : 300 : 100. After 2 hours, the as-synthesized submicron particles were collected by centrifugation and then washed with anhydrous methanol. After 2nd centrifugation, the particles were re-suspended in methanol prior to use. By doing this, the particle agglomeration occurring in the drying process can be avoided, as suggested in a report (26). The yield of ZIF-11 was about 90% on the basis of the amount of zinc element.

Membrane preparation

Fabrication of PEI Solution: Prior to use, PEI powder were dried overnight at 120 °C under vacuum and the desired polymer solution (15 wt.%) was prepared by dissolving a certain amount of PEI in NMP by stirring it for 24 h at room temperature until a clear uniform viscous solution was obtained.

Membrane Formation: Dense MMMs were prepared using the solution casting method. ZIF-11 particles were slurried into NMP solvent and sonicated 2 hours to obtain a homogenous dispersion. Ultrasonication Water Bath, VWR, was operated at 120 W and 40 Hz. After sonication, ZIF-11 particles stirred 1 day to fully disperse the fine powder. ZIF-11 crystals were first "primed" by adding a small amount, approximately 10 wt.% of the total PEI solution to the ZIF-11 mixture, after which the mixture was further stirred 2 hours and sonicated for another 30 min. Next, another 10 wt.% of PEI polymer was added into the solution. The suspension was stirred for 30 min and then bath sonicated for 30 min. After five additional iterations of stirring and sonication, the mixture was stirred overnight. Then, a final 30-min sonication period was completed before casting to remove any trapped air bubbles. After degassing the polymer solution, uniform films were cast on a glass plate by a film applicator. Mixed-matrix membranes were formed using 0-10-20-30 wt.% suspensions of ZIF-11 loadings in the polymer solution. The particle loadings of ZIF-11 particles in the MMMs were calculated based on the following equations (Eq. 1).

$$Particle\ \ loading\ \ wt.\% = \frac{Weight\ \ of\ \ particle}{(weight\ \ of\ \ particle + weight\ \ of\ \ polymer)} \times 100 \quad \textbf{(Eq. 1)}$$

Thermal annealing procedures: Membranes were cast on a glass plate using 400 µm film applicator. Thermal annealing of PEI MMMs membranes was conducted with a vacuum oven equipped with a temperature controller. Membranes were placed in the oven and heated to the required temperatures. After casting, the membranes were dried in the vacuum oven at 70 °C at 0.3 atm vacuum for at least 4 days to remove the solvent. Then, the dense films were formed and peeled off from the plate and placed into the vacuum oven to be further vacuum dried at 100 °C for 24 h and 120 °C for 24 h to remove any residual solvents. The membrane thickness was determined using RVS Micrometer. The resultant membranes had a thickness of 50±10 µm. The PEI and PEI-ZIF-11 mixed matrix membranes with a loading of 0-10-15-20-30 wt.% ZIF-11 was transparent with good flexibility as shown in Figure 3.

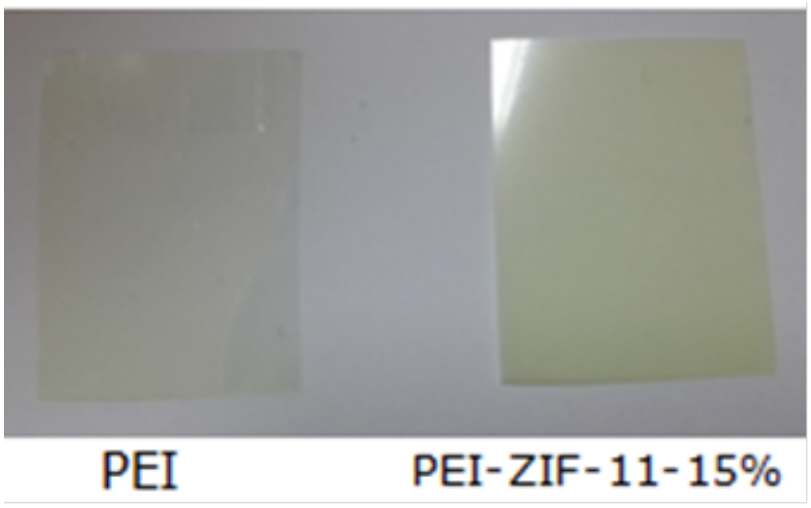

Figure 3. Image of PEI and PEI-ZIF-11-15% membranes.

Apparatus

The crystallographic structure of samples was analyzed using a Rigaku D/max-2200 Ultima X-ray diffractometer with CuKα radiation at a scan rate of 2θ = 0.01°/s from 2° to 40°. The accelerating voltage and applied current were 40 kV and 30 mA, respectively. Powder diffraction files (PDFs) from the International Centre of Diffraction Data (ICDD) in the Rigaku software (Rigaku, Japan) were used for qualitative phase analysis.

The number average mean size and size distributions of ZIF-11 particles were analyzed by a particle size analyzer (BI-90 Plus, Brookhaven Instruments Co.). The ZIF-11 particles were dispersed in methanol by means of an ultrasonic bath at room temperature and then quickly analyzed. In the dispersion process, no surfactants were used hence only submicrometer particles were suspended long enough to let particle size distribution be gathered.

The morphologies of ZIF-11 particles and PEI-ZIF-11 MMMs were analyzed by scanning electron microscopy. The SEM analyses were performed with a field-emission SEM (FEI-QUANTA FEG 450) attached with a METEK Energy Dispersive X-ray analyzer of silicon drift detector type.

FTIR spectra of the membranes was acquired on a Bruker Alpha-P ATR between 400 and 4000 cm^{-1}. The thermal stability of the ZIF-11 particles and PEI-ZIF-11 mixed matrix membranes were analyzed by thermogravimetric analysis (Perkin Elmer Pyris1 TGA) under flowing air from 25 °C to 1000 °C at a constant heating rate of 10 °C/min.

The glass transition temperatures (T_g) of the synthesized products were investigated by a Linseis DSC PT10 differential scanning calorimeter (DSC). A pre-conditioning procedure of heating up to 400 °C with 5 °C/min and natural cooling down to 30 °C was applied to all samples. Then in the second run, preconditioned samples (~10 mg) were heated up to 400 °C with a heating rate of 20 °C/min under N_2 atmosphere and the glass transition temperatures of the films were recorded.

The pure gas permeabilities were determined by constant volume and variable pressure method. Three gases (purity of 99.999%) having various kinetic diameters were used during this study; H_2 (2.89 Å), CO_2 (3.30 Å) and CH_4 (3.80 Å). All gases were used without further purification. 316 stainless steel gas permeation cell was custom designed and constructed for this study. The cell consisted of two parts, a permeate half and a feed half. The pressure built up was followed by means of vacuum pressure gauge, Leybold CTR 100 Ceravac 10 Torr. The values of change in the permeate pressure were collected on a local PC. The steady state slope of the downstream pressure vs. time was used to calculate permeability using the solution-diffusion model. Each test was started after the cell was pumped overnight. This enabled the evacuation of adsorbed water, gases and solvent. Each membrane was tested three times for each gas to determine reproducibility and the averages of three trials were reported along with one standard deviation. In each experiment, 2 cm^2 of membranes were cut and the ends were covered by aluminum tape to limit the gas permeation outside the reserved open area. Both sides of the cell were evacuated until a constant value of vacuum, approximately 10^{-3} atm was achieved. The retentate and permeate side pressures were equalized before switching to high pressure on the former side. Then, the feed pressure at retentate side was 4 bar and the testing temperature was 35 °C for all trials. The gas permeabilities were determined from the rate of downstream-pressure increase (dp/dt) obtained when permeation reached steady state according to the following equation (Eq. 2):

$$P = \frac{273.15\times10^{10}VL}{760AT((p_2\times76)/14.7)}\left(\frac{dp}{dt}\right) \qquad \textbf{(Eq. 2)}$$

where P is the permeability of the membrane to a gas and its unit is in Barrer (1 Barrer=1×10^{-10} cm3 (STP)-cm/cm^2s cmHg), V is the volume of the downstream chamber (cm^3) and L is the film thickness (cm). T is the experimental temperature (K), A assigns to the effective area of the membrane (cm^2) and the pressure of the feed gas in the upstream chamber is given by p_2 (psia).

The ideal separation factor of a membrane for gas A to gas B was evaluated as follows (Eq. 3):

$$\alpha_{A/B} = \frac{P_A}{P_B} \qquad \textbf{(Eq. 3)}$$

RESULTS AND DISCUSSION

Characterizations of ZIF-11 particles

Metal organic framework ZIF-11 was characterized via different methods. Figure 4a shows X-ray diffraction (XRD) pattern of ZIF-11 crystals by comparing with reported data (inset in Figure 4a) (27). The ZIF-11 crystals exhibited characteristic peaks (4.40°, 6.21°, 7.60°) well matched to the simulated ZIF-11 XRD pattern. ZIF-11 crystals with ideal inner structures had been successfully synthesized and Figure 4b showed the particle size analysis of ZIF-11 crystals. It was clear that size of the prepared ZIF-11 particles was mostly between 265 and 330 nm (an average of 280 nm) and ZIF-11 crystals had a narrow distribution of particle size based on DLS measurements. Figure 4c showed the typical FT-IR spectrum of ZIF-11 crystals (23). The ZIF-11 crystals showed characteristic absorption bands at 3088, 3057, 3032 cm^{-1} (=C–H stretching of aromatics), and 1611, 1465 cm^{-1} (C–C stretching in the aromatic ring). The bands occurring around 530–400 cm^{-1} were characteristic of ZnO molecules and were observed clearly in the ZIF-11 spectra (23). The band at 421 cm^{-1} corresponded to Zn–N stretching. Thereby, the above results confirmed the successful reaction of Zn^{2+} and benzimidazole in ZIF-11 crystals (28).

The thermal stability of the as-prepared ZIF-11 particles was investigated using TGA as shown in Figure 4d. The TGA curve of ZIF-11 yielded the first weight-loss of 2.8 wt.% between 130 and 200 °C corresponding to the loss of toluene (b.p.~110 °C) withheld in the particle cages. ZIF-11 particles were thermally stable up to 465 °C and then decomposed to form zinc oxide with a sharp weight loss at approximately 70% within the range of 465–830 °C. The residue at the end of the analysis (24.86 wt.%) was due to the oxidation of bound Zn metal to ZnO. Figure 4e showed the SEM image of ZIF-11 particles with a rhombic dodecahedron structure, which was consistent with the predicted one in the reported literatures (27,29). The average crystal size of ZIF-11 was about 280 nm with a size range of 0.2–1.5 μm (Figure 2e) as determined from SEM pictures. As seen in the SEM pictures in Figure 4e, it was observed that few large crystals as well as numerous smaller particles (~250-350 nm) exist together. In the DLS measurements, the number of average values were measured and it was highly likely that the larger ones than the reported particles were probably settled before the measurements were counted and recorded.

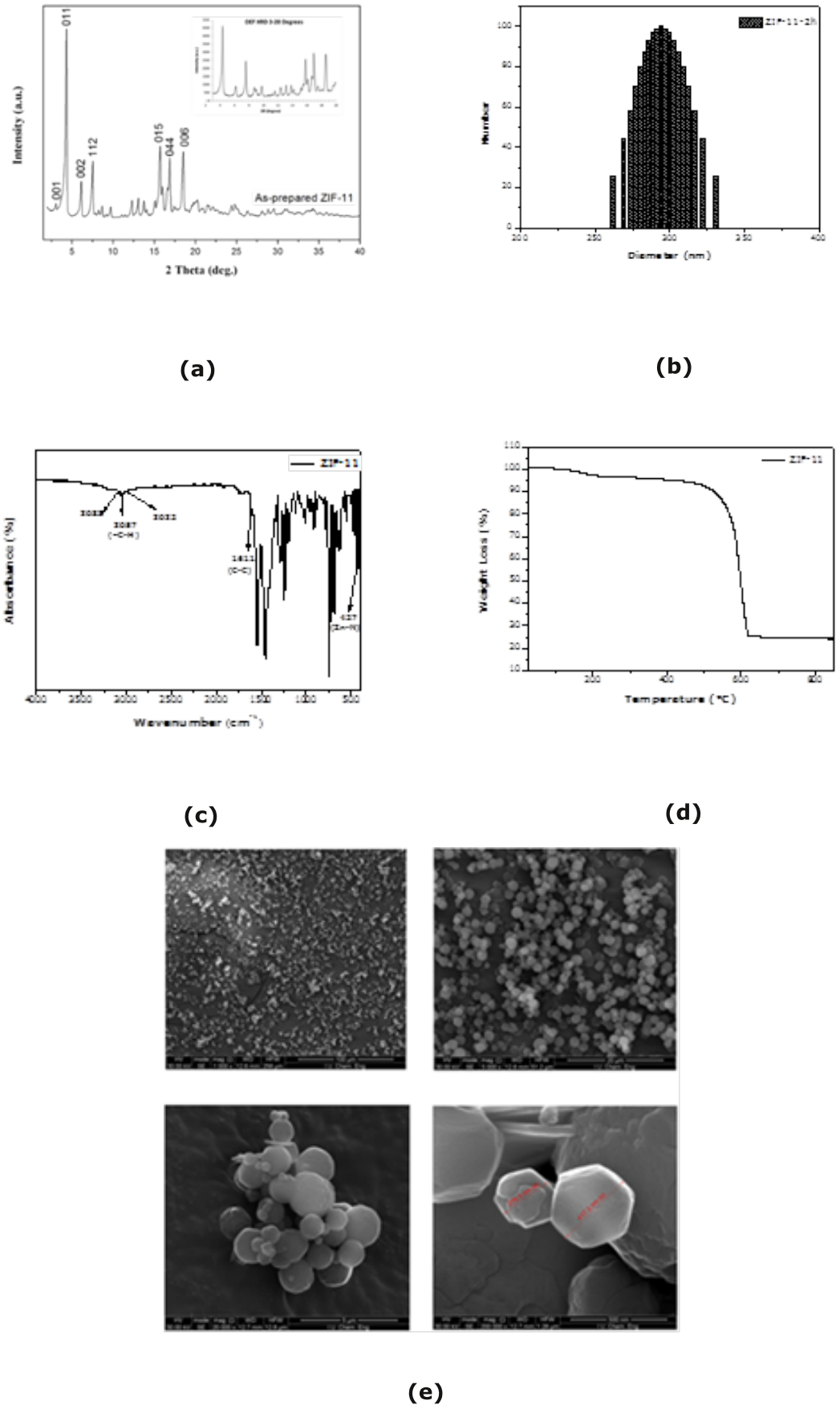

Figure 4. X-Ray diffraction pattern (a), the particle size distribution, (b), FT-IR spectrum (c), TG curve (d), and SEM image (e) of ZIF-11 crystals.

Characterizations of PEI-ZIF-11 mixed matrix membranes

Structural and thermal properties

Figure 5 showed the XRD patterns of pure PEI and PEI–ZIF-11 MMMs between 2° and 40° in order to determine their crystalline structures. The XRD pattern of pure PEI showed a broad amorphous peak of all the polyimides (30). From the XRD patterns of the MMMs (Figure 5) we can clearly observe a combination of the crystalline peaks of ZIF-11 and waved curve of pure PEI membrane. Thus, it was concluded that after the incorporation of MOF into PEI, ZIF-11 maintained its original structure integrity in the PEI-ZIF-11 MMMs. Pure ZIF-11 showed several sharp peaks (Figure 4a) while the main peak with highest intensity was around 2θ = 4.40°. Matching extremely well with pure ZIF-11 and PEI patterns (31). Furthermore, the intensity of characteristic peaks of ZIF-11 increased with accumulative ZIF-11 loading in MMMs. This finding showed that ZIF-11 crystalline structure remained unaffected after being embedded into the PEI matrix.

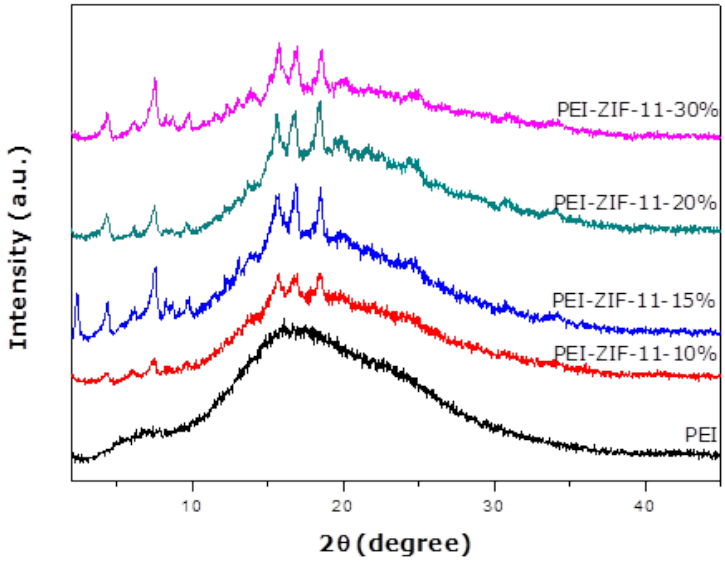

Figure 5. XRD patterns of PEI MMMs with different ZIF-11 loadings.

The FTIR spectra of pure PEI and PEI-ZIF-11 MMMs were shown in Figure 6. The FTIR spectra for the pure PEI membrane exhibited that characteristic absorption bands at 1779 cm^{-1}, 1718 cm^{-1} (asymmetric and symmetric C=O stretching vibration), 1240 cm^{-1} (Ar-O-Ar aromatic etheric stretching) and also vibrations at 1232, 777 cm^{-1} are characteristic adsorption peaks of polyetherimide structure (3,32). The ATR-FTIR spectra of PEI-ZIF-11 MMMs exhibited the features that was present in both ZIF-11 particles and a PEI film. Partial overlapping of the bands of the ZIF-11 crystals and PEI was also observed due to analogous chemical bonds (the presence of benzene rings in PEI and ZIF-11). The band occurring at 419 cm^{-1} was characteristic of Zn-N stretching and becoming more visible at 10, 15, 20, 30 wt.% loadings was a supplementary proof for the existence of ZIF-11 particles in the polymer matrix.

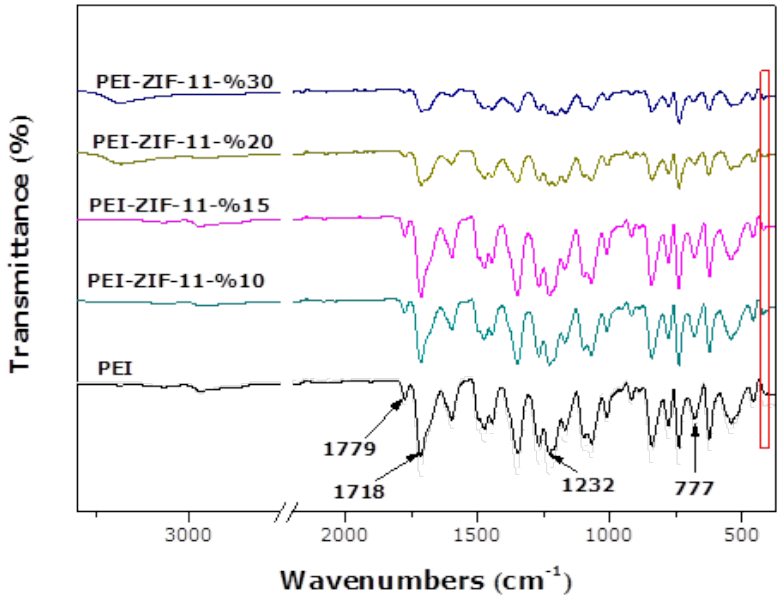

Figure 6. FTIR spectra of PEI-ZIF-11 (0-10-15-20-30 %) mixed matrix membranes.

SEM analysis was performed to investigate the structural morphology of the PEI-ZIF-11 mixed matrix membranes and the adhesion between ZIF-11 and PEI. Figure 7 showed the cross-section of pure PEI membrane (Figure 7a) and cross-sections of PEI-ZIF-11 MMMs containing 20 wt.% of ZIF-11 particles (Figure 7b-c-d), respectively. The pure PEI membrane showed a dense morphology without any visible deformation. Mixed matrix membrane morphology of dispersed phase strongly influenced the gas transport properties. Cross-sectional SEM images of the PEI-ZIF-11 MMMs were acquired to probe the dispersion of particles in the polymer matrix. The SEM images of MMMs showed good dispersion of the ZIF-11 particles throughout the polymer matrix. Any defect or agglomerates of ZIF-11 particles were not observed in the cross-sectional surfaces of the PEI-ZIF-11 MMM. On the other hand, the concentric cavities in the MMMs (Figure 7b, c and d) indicated a strong interfacial interaction between the PEI polymer and the ZIF-11 particles (14). The ZIF-11 crystals were completely enfolded by a polymer film as seen in Figure 7. Comparing MMMs with pure PEI membrane, a flat and homogenous structure was transformed into a crater-like structure in homogeneous pattern upon addition of ZIF-11 in the matrix (29). Formation of the crater-like morphology was due to de-bonding of added particles to polymeric matrix during freeze fracturing.

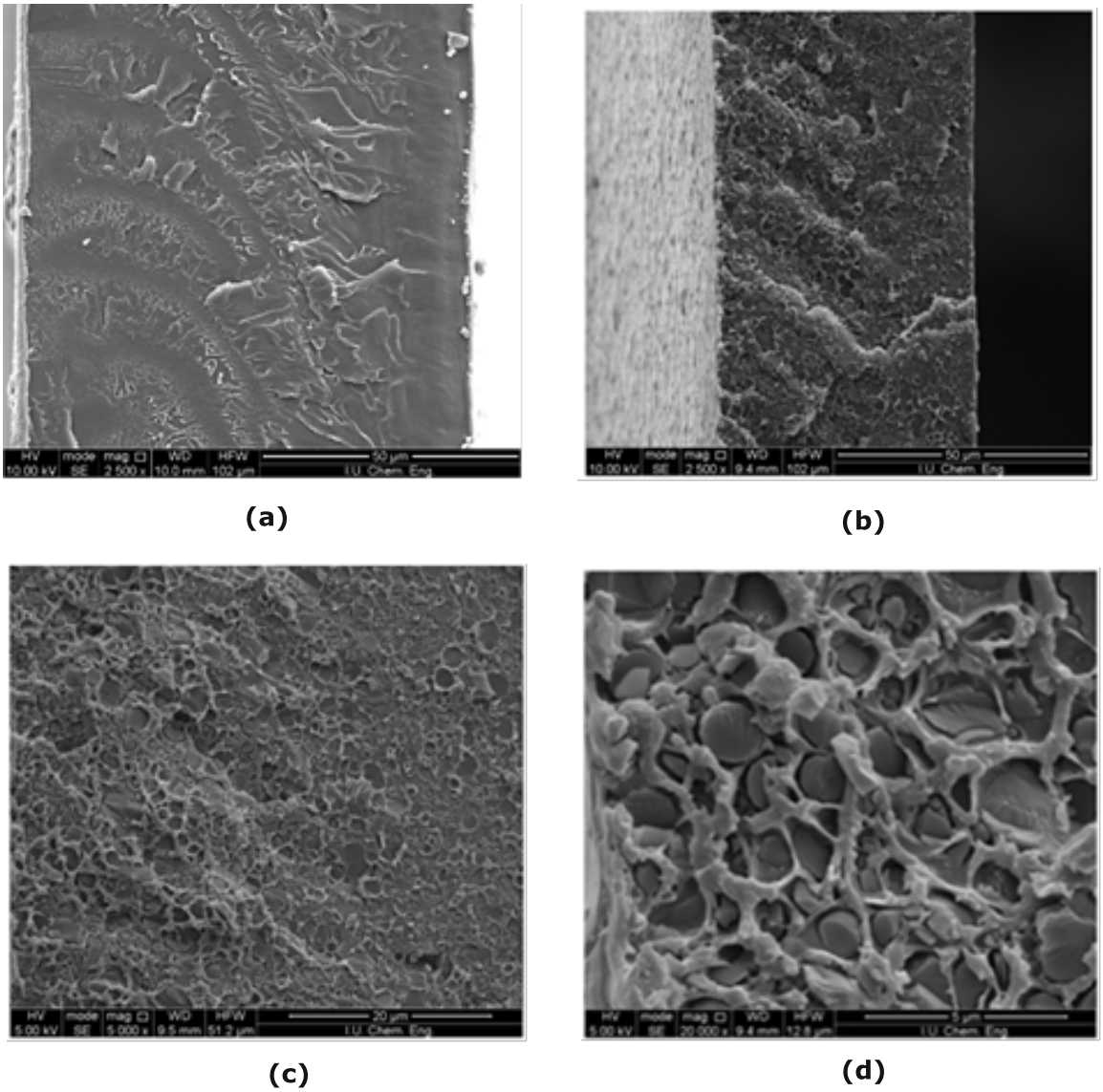

Figure 7. Cross-sectional SEM images of (a) PEI, (b-c-d) PEI-ZIF-11-20 wt.%.

TGA analysis was also carried out to determine the thermal degradation of all MMMs as a function of temperature and to study the effect of ZIF-11 on thermal stability of the membranes. The TGA curves for PEI-ZIF-11 MMMs were shown in Figure 8. The PEI membrane exhibited a two-step degradation pattern whereas the PEI-ZIF-11 MMMs exhibited a three-step degradation pattern. In the curve of the PEI membrane, first weight loss occurred between 150 and 300 °C, corresponding to the weight loss of the NMP solvent on the PEI matrix. The major weight loss observed at 567.25 °C was attributed to the complete decomposition of the polymer.

For PEI-ZIF-11 MMMs, three peaks associated with three weight loss stages were illustrated in Figure 8. The first weight loss rate for neat PEI, PEI-ZIF-11 (10 wt.%), PEI-ZIF-11 (15 wt.%), PEI-ZIF-11 (20 wt.%) and PEI-ZIF-11 (30 wt.%) up to 300 °C is 3.28, 6.12, 6.15, 7.32 and 7.27%, respectively (Table 3). Similar to the PEI membrane, the peaks between 152 and 307 °C correspond to some residual solvent in ZIF-11 and the polymer matrix. The weight loss corresponding to the second peak was attributed to the decomposition of organic groups into the MMMs matrix. The final weight loss is associated with the structural decomposition of the ZIF-11 groups to give residual ZnO and carbonaceous species. The thermal degradation of the ZIF-11 alone started around 465 °C (Figure 4d). The addition of the ZIF-11 into the polymer matrix slightly decreased the stability of the pure PEI membranes, possibly due to the fact that the ZIF-11 might have catalyzed the polymer degradation. The thermal stability of these composites was still preserved mostly up to 460 °C. This high thermal stability was acceptable for PEI-based materials in many applications.

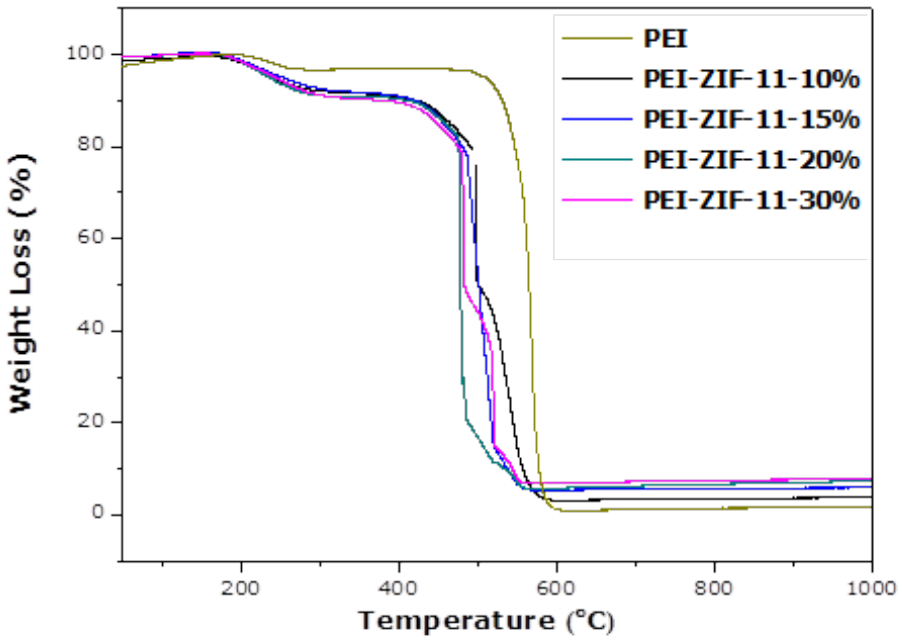

Figure 8. TGA analysis of PEI-ZIF-11 mixed matrix membranes in air atmosphere.

Table 3. TGA and DSC results of PEI-ZIF-11 MMMs.

Membrane	Weight loss (%) 200 - 300°C	Residue (%) 900°C	T_g (°C)
PEI	3.28	1.60	210.5
PEI-ZIF-11-10%	6.12	3.66	217.0
PEI-ZIF-11-15%	6.53	5.83	218.5
PEI-ZIF-11-20%	7.32	7.04	219.0
PEI-ZIF-11-30%	7.27	7.99	217.5

The influence of the addition of ZIF-11 particles on the glass transition temperature (T_g) of PEI-ZIF-11 MMMs, was illustrated in Table 3. There were some changes in the T_g of the MMMs relative to the pure polymer. The DSC result of neat PEI film indicated its T_g value as 210.5 °C. T_g values of MMMs showed that by increasing ZIF-11 loading in the MMMs, their T_g values increased and shifted from 210.5 °C to 219.0 °C once ZIF-11 loading reached 20 wt.%. By adding more ZIF-11, free volume of the polymer chain reduced due to the progressively increasing association of polymer chains to the ZIF-11 surface and/or their entrance into the ZIF-11 pores. These interactions between polymer chains and incorporated ZIF-11 restricted the movement of the polymer chains and this restriction in movement resulted in higher T_g values of MMMs (33). Clearly, this increased T_g values were an indication of interactions between ZIF-11 and PEI at a molecular level.

Gas Separation properties

Gas separation properties of pure PEI membrane and PEI-ZIF-11 MMMs with various ZIF-11 loadings were tested to investigate the influences of ZIF-11 on the MMMs. Permeability measurements for H_2, CO_2 and CH_4 at various ZIF-11 loadings (0-10-15-20-30 wt.%) into PEI membrane films were carried out and listed in Table 4. Also, CO_2/CH_4, H_2/CO_2 and H_2/CH_4 ideal selectivities were calculated from the single gas permeability results. The permeance measurements were performed at 35 °C and to assess reproducibility, at each percentage of loading experiments was repeated at least three times. The error of the measurements was calculated as the standard deviation percentage [(standard deviation / average) x 100].

Figure 9 showed the gas separation performance of PEI and PEI-ZIF-11 MMMs incorporating ZIF-11 particles. The gas separation performance of the pure PEI membrane achieved in this study was found to be consistent with the values reported in the literature (34). In the pure PEI membrane, the gas permeation fluxes for H_2, CO_2, and CH_4 pure gases were found to be 6.30, 1.36, and 0.187 Barrer, respectively. The CO_2/CH_4, H_2/CO_2, and H_2/CH_4 ideal gas pair selectivities were found to be 7.27, 4.63, and 33.69, respectively.

The incorporation of ZIF-11 particles evidently increased the gas permeation of H_2, CO_2, and CH_4 pure gases and CO_2/CH_4, and H_2/CH_4 ideal gas selectivity of the membranes. It can be seen from Table 4 that the PEI-ZIF-11 MMMs exhibited higher selectivity and permeability than the pure PEI membranes. For example, incorporation of 20 wt.% of ZIF-11 to PEI resulted in ~330% increase in H_2 permeability, while permeabilities of CH_4 and CO_2 were increased by ~71% and 80%, respectively. The reason for the permeability enhancement on MMMs was thought to be due to that ZIF-11 particles provided well-aligned channels within polymer to facilitate the permeation. On the other hand, as stated in the previous sections, the average pore size of ZIF-11 was approximately 3.0 Å which permitted the transport of gas molecules with smaller kinetic diameter (such as, H2, 2.89 Å) and partially block the large molecules (such as CH_4, 3.8 Å). ZIF-11 had naturally the most promising pore dimensions with window cut-offs ranging between 3.08 and 3.10 Å, which were ideal for hydrogen sieving applications. However, sharp size selectivity for gases with a bigger diameter than the pore size of ZIF-11 was not observed owing to the flexibility of the ZIF-11 framework (19). Thus, flexibility significantly affected the diffusion of large gas molecules in the narrow pored materials. CO_2 and CH_4 were also able to get adsorbed in ZIF-11 because of aperture flexibility of ZIF-11. On the other hand, the increase in permeability may be due to both intermitted chain packing in polymer matrix by the dispersed phase in polymer-phase and also the presence of the porous ZIF-11 (35).

From Figure 9, at the 30 wt.% ZIF-11 loading, the permeability of all gases was also decreased significantly relative to the 20 wt.% loading, However, the permeability was still higher than the pristine PEI membrane. The decrease in permeability at the higher loading values can be interpreted due to high ratio of ZIF-11 which played as barrier across the gas diffusion path on polymer. A reduction in permeability with the introduction of inorganic particles to polymer membranes has also been observed by other researchers. Ordonez et al. reported that the higher percentage of ZIF particles in the MMM reduced the amount of polymer available area for gas transport. Also, higher ZIF loading was increased the diffusion path length for the gases as they were constrained to take a more tortuous path around the ZIF particles, and likely increased the density of the remaining polymer chains thereby reducing free volume in the membrane (36). Moore et al. also explained this phenomenon well as Case I or Case V (37). These membranes exhibited some increases in selectivity while similar decreases in permeability observed, compared to the neat polymer.

Moreover, the above observations may also be attributed to the interaction between ZIF-11 particles and the PEI polymer, which was due to the affinity of the organic linkers in ZIF-11 to the PEI chains and also the coordination of some unsaturated metal ions in MOFs to carbonyl groups in the PEI chains.

In conclusion, the results were interpreted as no voids or large channels were present in the polymer and ZIF-11 interface, because such voids and channels would have resulted in a continuing increase in the permeabilities of H_2, CO_2 and CH_4 as the ZIF-11 loading increased to higher values. The results for MMMs also validated by the SEM images that showed no significant voids at the polymer/filler interface. This change in the trend also put forward as an indirect evidence that the mixed matrix membranes were defect free and the interaction between the ZIF-11 particles and the polymer played a role in gas permeation mechanism.

The experimental results were shown in Robeson's trade-off plot in Figure 10 and Figure 11. Adding ZIF-11 particles to the polymer matrix resulted in the performances closer to the Robeson upper bound due to enhancement of H_2 permeability and selectivity. The pure gas permeation results of the pristine PEI membrane were just placed below the upper bound, whereas the gas permeation results of MMMs gathered near the upper bound, particularly for PEI-ZIF11–30% and PEI-ZIF11–20% MMMs. These results indicated that ZIF-11 had the vast potential of separating H_2/CH_4 and CO_2/CH_4 mixture due to high H_2 selectivity of ZIF-11 particles.

Table 4. Gas permeability values (Barrer) of the pure PEI and PEI-ZIF-11 MMMs at 35°C and 4 bar.

Membrane	**Permeability (Barrer)**			**Ideal Selectivity**		
	$P(H_2)$	**$P(CH_4)$**	**$P(CO_2)$**	**$\alpha_{(CO2/CH4)}$**	**$\alpha_{(H2/CO2)}$**	**$\alpha_{(H2/CH4)}$**
PEI	6.30 ± 0.070	0.187 ± 0.050	1.36 ± 0.080	7.27	4.63	33.69
PEI-ZIF-11-10%	7.38 ± 0.290	0.19 ± 0.008	1.54 ± 0.120	8.10	4.79	38.84
PEI-ZIF-11-15%	20.73 ±0.600	0.25 ± 0.002	4.63 ± 0.300	18.52	4.47	82.92
PEI-ZIF-11-20%	27.10 ±1.200	0.32 ± 0.007	6.95 ± 0.770	21.18	3.89	84.68
PEI-ZIF-11-30%	8.70 ± 0.330	0.048 ± 0.017	2.73 ± 0.107	56.87	3.18	181.25

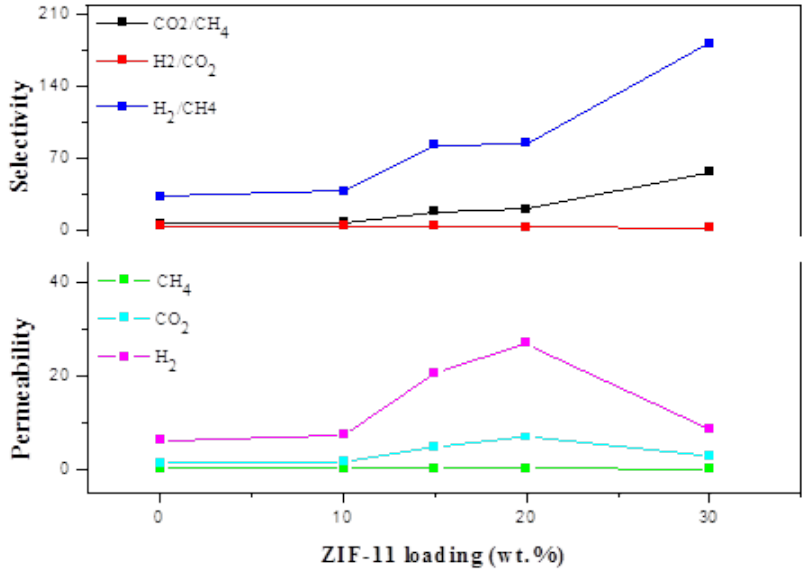

Figure 9. Enhancement of gas transport properties for H_2, CH_4, and, CO_2 as a function of ZIF-11 loading in PEI-ZIF-11 MMMs.

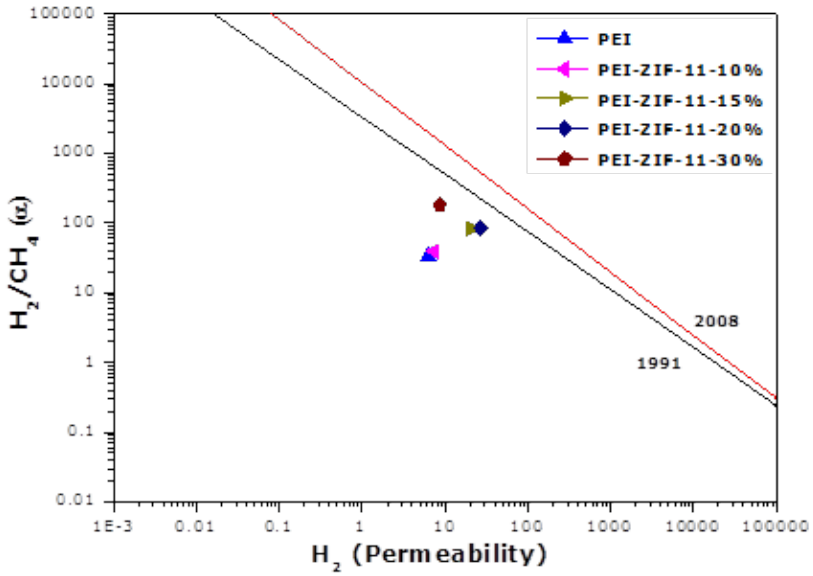

Figure 10. Comparison of pure and mixed H_2/CH_4 separation performance of PEI-ZIF-11 MMMs with the upper bound.

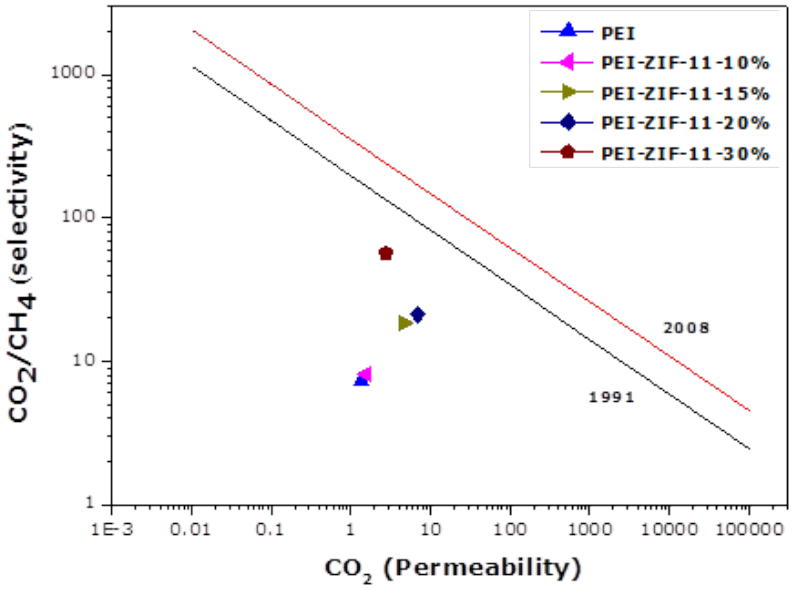

Figure 11. Comparison of pure and mixed CO_2/CH_4 separation performance of PEI-ZIF-11 MMMs with the upper bound.

The influence of MOF particles in MMMs for H_2, CO_2, and CH_4 gases separations was studied by preparing dense and asymmetric PEI membrane filled with various ZIF-11 loading. A zeolitic imidazolate framework, ZIF-11, was successfully synthesized, characterized, and evaluated as a potential adsorbent for H_2/CH_4 and CO_2/CH_4 separation. The priming protocol to prepare the MMMs resulted in a good distribution of fillers in the polymer matrix even under high loading. The XRD pattern of the MMMs showed that ZIF-11 maintained its crystallinity through and after the heating processes in the membrane preparation procedure. FTIR and TGA analysis showed interaction of ZIF-11 samples with PEI polymer. Both the selectivity and permeability for H_2/CH_4 and CO_2/CH_4 were increased by inclusion of ZIF-11 particles (up to 20 wt.% loading). At high loading of the ZIF-11 particles, the selectivity was further increased but the permeability was reduced. The increase in selectivity interpreted as the absence of voids at the PEI–ZIF-11 interface. This was confirmed by the SEM image of the membrane cross-section. The incorporation of ZIF-11 particles in the PEI matrix, can lead to an overall improvement in performance of permeability and selectivity. In the literature, Lunxi *et al.* studied ZIF-11/PBI composite membranes and tested gas separation performances of membranes for H_2 and CO_2 gases at room temperature. They obtained H_2/CO_2 ideal selectivity of 5.6 for 16.1 wt. % ZIF-11/PBI composite membrane (38). Coronas *et al.* synthesized nano-sized ZIF-11/Matrimid MMMs and investigated selectivity and permeability of H_2/CO_2 in MMMs. They showed that 25 wt.% ZIF-11 MMM showed improvement in H_2/CO_2, with a H_2/CO_2 separation selectivity of 4.4 at 35 °C (22). On the other hand, Lunxi and Coronas did not test the gas separation performance of membranes for CH_4 gas. Finally, the selectivity of H_2/CH_4 was achieved equal to 181.25. The results confirmed that PEI was a suitable candidate for hydrogen separation membranes.

ACKNOWLEDGMENTS

This work was supported in part by the Scientific and Technological Research Council of Turkey (TUBITAK) through [Grant no. 113M278].

REFERENCES

1. Zornoza B, Tellez C, Coronas J, Gascon J, Kapteijn F. Metal organic framework based mixed matrix membranes: An increasingly important field of research with a large application potential. Microporous Mesoporous Mater. 2013;166:67–78. DOI: 10.1016/j.micromeso.2012.03.012.

2. Sanders DF, Smith ZP, Guo R, Robeson LM, McGrath JE, Paul DR, et al. Energy-efficient polymeric gas separation membranes for a sustainable future: A review. Vol. 54, Polymer (United Kingdom). 2013. p. 4729–61. DOI: 10.1016/j.polymer.2013.05.075.

3. Arjmandi M, Pakizeh M. Mixed matrix membranes incorporated with cubic-MOF-5 for improved polyetherimide gas separation membranes: Theory and experiment. J Ind Eng Chem. 2014;20(5):3857–68. DOI: 10.1016/j.jiec.2013.12.091.

4. Bastani D, Esmaeili N, Asadollahi M. Polymeric mixed matrix membranes containing zeolites as a filler for gas separation applications: A review. Vol. 19, Journal of Industrial and Engineering Chemistry. 2013. p. 375–93. DOI: 10.1016/j.jiec.2012.09.019.

5. Robeson LM. The upper bound revisited. J Memb Sci. 2008;320(1-2):390–400. DOI: 10.1016/j.memsci.2008.04.030.

6. Keser Demir N, Topuz B, Yilmaz L, Kalipcilar H. Synthesis of ZIF-8 from recycled mother liquors. Microporous Mesoporous Mater. 2014;198:291–300. DOI: 10.1016/j.micromeso.2014.07.052.

7. Dorosti F, Omidkhah M, Abedini R. Fabrication and characterization of Matrimid/MIL-53 mixed matrix membrane for CO2/CH4 separation. Chem Eng Res Des. 2014;92(11):2439–48. DOI: 10.1016/j.cherd.2014.02.018.

8. Hu T, Dong G, Li H, Chen V. Effect of PEG and PEO-PDMS copolymer additives on the structure and performance of Matrimid hollow fibers for CO2 separation. J Memb Sci. 2014;468:107–17. DOI: 10.1016/j.memsci.2014.05.024.

9. Chen XY, Vinh-Thang H, Rodrigue D, Kaliaguine S. Amine-Functionalized MIL-53 Metal-Organic Framework in Polyimide Mixed Matrix Membranes for CO2/CH4 Separation. Ind Eng Chem Res. 2012;51(19):6895–906. DOI: 10.1021/Ie3004336.

10. Dai Y, Johnson JR, Karvan O, Sholl DS, Koros WJ. Ultem ??/ZIF-8 mixed matrix hollow fiber membranes for CO 2/N 2 separations. J Memb Sci. 2012;401-402:76–82. DOI: 10.1016/j.memsci.2012.01.044.

11. Nevruzoglu V, Demir S, Karaca G, Tomakin M, Bilgin N, Yilmaz F. Improving the stability of solar cells using metal–organic frameworks. J Mater Chem A. 2016;4:7930–5. DOI: 10.1039/C6TA02609E.

12. Demir S, Çepni HM, Topcu Y, Holynska M, Keskin S. A phytochemical-containing metal–organic framework: Synthesis, characterization and molecular simulations for hydrogen adsorption. Inorganica Chem Acata. 2015;427:138–43. DOI: 10.1016/j.ica.2014.12.010.

13. Günay G, Yeşilel OZ, Erer H, Keskin S, Tabak A. A zinc(II) metal organic framework based on flexible o-phenylenediacetate and rigid 4,4′-azobis(pyridine) ligands: Synthesis, crystal structure and hydrogen gas adsorption property. Polyhedron. 2015;100:108–13. DOI: 10.1016/j.poly.2015.07.017.

14. Basu S, Cano-Odena A, Vankelecom IFJ. MOF-containing mixed-matrix membranes for CO2/CH4 and CO2/N2 binary gas mixture separations. Sep Purif Technol. 2011;81(1):31–40. DOI: 10.1016/j.seppur.2011.06.037.

15. Erucar I, Keskin S. Computational screening of metal organic frameworks for mixed matrix membrane applications. J Memb Sci. 2012;407-408:221–30. DOI: 10.1016/j.memsci.2012.03.050.

16. Askari M, Chung T-S. Natural gas purification and olefin/paraffin separation using thermal cross-linkable co-polyimide/ZIF-8 mixed matrix membranes. J Memb Sci. 2013;444:173–83. DOI: 10.1016/j.memsci.2013.05.016.

17. Yilmaz G, Keskin S. Predicting the Performance of Zeolite Imidazolate Framework/Polymer Mixed Matrix Membranes for CO2 , CH4 , and H2 Separations Using Molecular Simulations. Ind Eng Chem Res. 2012;51(43):14218–28. DOI: 10.1021/ie302290a.

18. Morris W, He N, Ray KG, Klonowski P, Furukawa H, Daniels IN, et al. A combined experimental-computational study on the effect of topology on carbon dioxide adsorption in zeolitic imidazolate frameworks. J Phys Chem C. 2012;116(45):24084–90. DOI: 10.1021/jp307170a.

19. Wijenayake SN, Panapitiya NP, Versteeg SH, Nguyen CN, Goel S, Balkus KJ, et al. Surface cross-linking of ZIF-8/polyimide mixed matrix membranes (MMMs) for gas separation. Ind Eng Chem Res. 2013;52(21):6991–7001. DOI: 10.1021/ie400149e.

20. Assfour B, Leoni S, Seifert G. Hydrogen adsorption sites in zeolite imidazolate frameworks ZIF-8 and ZIF-11. J Phys Chem C. 2010;114(31):13381–4. DOI: 10.1021/jp101958p.

21. Banerjee R, Phan A, Wang B, Knobler C, Furukawa H, O'Keeffe M, et al. High-throughput synthesis of zeolitic imidazolate frameworks and application to CO2 capture. Science. 2008;319(5865):939–43. DOI: 10.1126/science.1152516.

22. Sanchez-Lainez J, Zornoza B, Mayoral A, Berenguer-Murcia Á, Cazorla-Amorós D, Tellez C, et al. Beyond the H2/CO2 upper bound: one-step crystallization and separation of nano-sized ZIF-11 by centrifugation and its application in mixed matrix membranes. J Mater Chem A. 2015;7:6549–56. DOI: 10.1039/C4TA06820C.

23. He M, Yao J, Liu Q, Zhong Z, Wang H. Toluene-assisted synthesis of RHO-type zeolitic imidazolate frameworks: synthesis and formation mechanism of ZIF-11 and ZIF-12. Dalton Trans. 2013;42(47):16608–13. DOI: 10.1039/c3dt52103f.

24. Shamsabadi AA, Kargari A, Babaheidari MB, Laki S, Ajami H. Role of critical concentration of PEI in NMP solutions on gas permeation characteristics of PEI gas separation membranes. J Ind Eng Chem. 2013;19(2):677–85. DOI: 10.1016/j.jiec.2012.10.006.

25. Park KS, Ni Z, Cote AP, Choi JY, Huang R, Uribe-Romo FJ, et al. Exceptional chemical and thermal stability of zeolitic imidazolate frameworks. Proc Natl Acad Sci U S A. 2006;103(27):10186–91. DOI: 10.1073/pnas.0602439103.

26. Cravillon J, Monzer S, Lohmeier SJ, Feldhoff A, Huber K, Wiebcke M. Rapid room-temperature synthesis and characterization of nanocrystals of a prototypical zeolitic imidazolate framework. Chem Mater. 2009;21(8):1410–2. DOI: 10.1021/cm900166h.

27. Thorkelson J. A Study of the Synthesis of the Zeolitic Imidazolate Framework Membrane Zif-11. Texas A&M University; 2011. Available from: http://oaktrust.library.tamu.edu/bitstream/handle/1969.1/148789/Thorkelson1.pdf?sequence=1.

28. Hu H, Liu S, Chen C, Wang J, Zou Y, Lin L, et al. Two novel zeolitic imidazolate frameworks (ZIFs) as sorbents for solid-phase extraction (SPE) of polycyclic aromatic hydrocarbons (PAHs) in environmental water samples. Analyst. 2014;139(22):5818–26. DOI: 10.1039/C4AN01410C .

29. Ahmad J, Hägg MB. Development of matrimid/zeolite 4A mixed matrix membranes using low boiling point solvent. Sep Purif Technol. 2013;115:190–7. DOI: 10.1016/j.seppur.2013.04.049.

30. Koley T, Bandyopadhyay P, Mohanty AK, Banerjee S. Synthesis and characterization of new aromatic poly(ether imide)s and their gas transport properties. Eur Polym J. 2013;49(12):4212–23. DOI: 10.1016/j.eurpolymj.2013.10.001.

31. Perez E V., Balkus KJ, Ferraris JP, Musselman IH. Metal-organic polyhedra 18 mixed-matrix membranes for gas separation. J Memb Sci. 2014;463:82–93. DOI: 10.1016/j.memsci.2014.03.045.

32. Namvar-Mahboub M, Pakizeh M. Development of a novel thin film composite membrane by interfacial polymerization on polyetherimide/modified SiO2 support for organic solvent nanofiltration. Sep Purif Technol. 2013;119:35–45. DOI: 10.1016/j.seppur.2013.09.003.

33. Khosravi T, Mosleh S, Bakhtiari O, Mohammadi T. Mixed matrix membranes of Matrimid 5218 loaded with zeolite 4A for pervaporation separation of water-isopropanol mixtures. Chem Eng Res Des. 2012;90(12):2353–63. DOI: 10.1016/j.cherd.2012.06.005.

34. Takahashi S, Paul DR. Gas permeation in poly(ether imide) nanocomposite membranes based on surface-treated silica. Part 1: Without chemical coupling to matrix. Polymer (Guildf). 2006;47(21):7519–34. DOI: 10.1016/j.polymer.2006.08.029.

35. Nafisi V, Hägg MB. Development of dual layer of ZIF-8/PEBAX-2533 mixed matrix membrane for CO2 capture. J Memb Sci. 2014;459:244–55. DOI: 10.1016/j.seppur.2014.03.006.

36. Ordonez MJC, Balkus KJ, Ferraris JP, Musselman IH. Molecular sieving realized with ZIF-8/Matrimid?? mixed-matrix membranes. J Memb Sci. 2010;361(1-2):28–37. DOI: 10.1016/j.memsci.2010.06.017.

37. Moore TT, Koros WJ. Non-ideal effects in organic-inorganic materials for gas separation membranes. J Mol Struct. 2005;739(1-3):87–98. DOI: 10.1016/j.molstruc.2004.05.043.

38. Li L, Yao J, Wang X, Cheng YB, Wang H. ZIF-11/Polybenzimidazole composite membrane with improved hydrogen separation performance. J Appl Polym Sci. 2014;131(22):41056. DOI: 10.1002/app.41056.

Research article

Türkçe öz ve anahtar kelimeler

POLİETERİMİD (PEI)/ZEOLİTİK İMİDAZOLAT (ZIF-11) KARIŞIMI MATRİS MEMBRANLARIN YAPISAL KARAKTERİZASYONU VE GAZ GEÇİRME ÖZELLİKLERİ

Bu çalışmada, polieterimid (PEI-Ultem1000)/ZIF-11 karışık matris membranlarının hazırlanması ve farklı oranlarda ZIF-11 partikülleri (ağırlıkça % 0, 10, 15, 20, ve 30) yüklenmesinin etkisi incelenmiştir. Ortalama partikül boyutu ~280 nm olarak sentezlenen ZIF-11 partikülleri PEI membranına katkısı ile karışık matris membranlar (KMM) hazırlanmıştır. ZIF-11 yüklemesinin gaz ayırma performansına etkisi H_2, CO_2 ve CH_4 gazları için 35 °C ve 4 bar basınçta incelenmiştir. ZIF-11 yüklemesindeki artış ile KMM'lerin gaz geçirgenlik özellikleri artmıştır. %20 ZIF-11 yüklemesinde H_2 ve CO_2 gazlarının geçirgenlik katkısız polimere göre dört kat artmıştır. CH_4 geçirgenliğinde ise bir miktar artış gözlenmiştir. Ağırlıkça %20'nin üzerinde ZIF-11 yüklemesinde, bütün gazlar için geçirgenlik değerleri düşerken CO_2/CH_4 ve H_2/CH_4 seçicilikleri ZIF-11 yüklemesine bağlı olarak artmıştır.

Anahtar Kelimeler: Karışık matris membranlar, zeolit imidazolat kafesler, polieterimid, gaz ayırma.
Gonderme: 28 Mayıs 2016, **Düzeltme:** 24 Haziran 2016, **Kabul:** 28 Haziran 2016.